First Light of the ESO Laser Guide Star Facility

D.Bonaccini Calia[a], E. Allaert[a], J.L.Alvarez[a], C. Araujo Hauck[a], G.Avila[a], E.Bendek[a], B. Buzzoni[a], M. Comin[a], M. Cullum[a], R.Davies[b], M. Dimmler[a], I.Guidolin[a], W. Hackenberg[a], S.Hippler[c], S.Kellner[b], A. van Kesteren[a], F. Koch[a], U.Neumann[c], T.Ott[b], D. Popovic[a], F.Pedichini[d], M Quattri[a], J. Quentin[a], S.Rabien[b], A.Silber[a] and M.Tapia[a]

[a]*European Southern Observatory,*
Karl-Schwarzschild-Str. 2, D-85748 Garching, Germany

[b]*Max-Planck-Institut für Extraterrestrische Physik,*
Giessenbachstraße, D- 85748 Garching, Germany

[c] *Max-Planck-Institut für Astronomie, Königstuhl 17, D-69117 Heidelberg, Germany*

[d] *Osservatorio Astronomico di Roma, Via di Frascati 33, I-00040 Monte Porzio Catone, Italy*

1 Abstract

Two teams of scientists and engineers at Max Planck Institut fuer Extraterrestrische Physik and at the European Southern Observatory have joined forces to design, build and install the Laser Guide Star Facility for the VLT.

The Laser Guide Star Facility has now been completed and installed on the VLT Yepun telescope at Cerro Paranal. In this paper we report on the first light and first results from the Commissioning of the LGSF.

Keywords: Sodium Laser Guide-Star, Adaptive Optics, Dye Lasers

2 INTRODUCTION

The ESO Laser Guide Star Facility (LGSF) has been designed and built by a collaborative effort between the Max Planck Institut für Extraterrestrische Physik, the Max Planck Institut für Astronomie and the European Southern Observatory.

Starting with integration on the UT4 telescope in November 2005, the project has reached the First Light milestone on the VLT on January 28th 2006, 5 years after the start of the collaboration. In this paper we report on the First Light performances. To our knowledge this is the shortest time taken to build and bring to operation a LGSF for astronomy. It is now undergoing commissioning phases, in order to be offered to the astronomical community in the ESO period 78, in service mode.

The Keck Observatory has shown reliable and steady operation of LGS-AO systems. Our LGSF system wants to make a step forward in solving operational issues which have made so far LGS-AO intense in terms of required support and manpower. To this end we have designed the system with the following technical rationale:

Advances in Adaptive Optics II, edited by Brent L. Ellerbroek, Domenico Bonaccini Calia,
Proc. of SPIE Vol. 6272, 627207, (2006) · 0277-786X/06/$15 · doi: 10.1117/12.674484

1. Use a CW dye laser (PARSEC), with automatic servo-controls in order to allow remote operation and service once/week;
2. Use a single mode fibre relay in order to simplify the laser beam transfer and preserve the diffraction limited performace;
3. Use a diffraction limited Launch telescope in order to minimize the LGS size and optimize the use of the laser power;
4. Build the Laser Guide Star system as a Facility of the VLT UT4 (Yepun) telescope, to be used automatically by the AO systems.

3 LGSF TOP LEVEL REQUIREMENTS

The principal (or top level) requirements for the LGSF are:

- Monostatic projection (i.e. centered on the UT4 pupil, launch telescope behind M2).
- The laser source is continuous-wave at 589 nm (D2 line), 1 GHz max linewidth
- LGS return flux ≥ 1.0 × 106 ph/s/m2 @ Nasmyth focus
- LGS spot size ≤ 1.25” FWHM (with 0.65” seeing at 0.55 µm, 45° Zenith distance)
- LGS residual position jitter ≤ 0.09 arcsec rms in closed loop
- LGSF is operable at UT zenith distances ≤ 60°,
- LGS with 20” pointing radius from UT4 centerfield
- Operation done by trained night assistants, with standby and on-line modes changed via software, no intervention on the LGSF required before or during the observing night.
- Regular maintenance at intervals of once/week
- Class IV laser and Observatory Safety and Engineering standards have to be observed

4 LGSF DESIGN AND SUBSYSTEMS

The LGSF is composed of five main subsystems:

- The Laser Clean Room
- The PARSEC dye laser
- The Beam Relay System Input, which arranges the laser beam spectral and spatial formats to enter stably in the single mode PCF
- The fibre relay system, based on the Photonic Crystal Fiber
- The Launch Telescope, with its Beam diagnostics devices

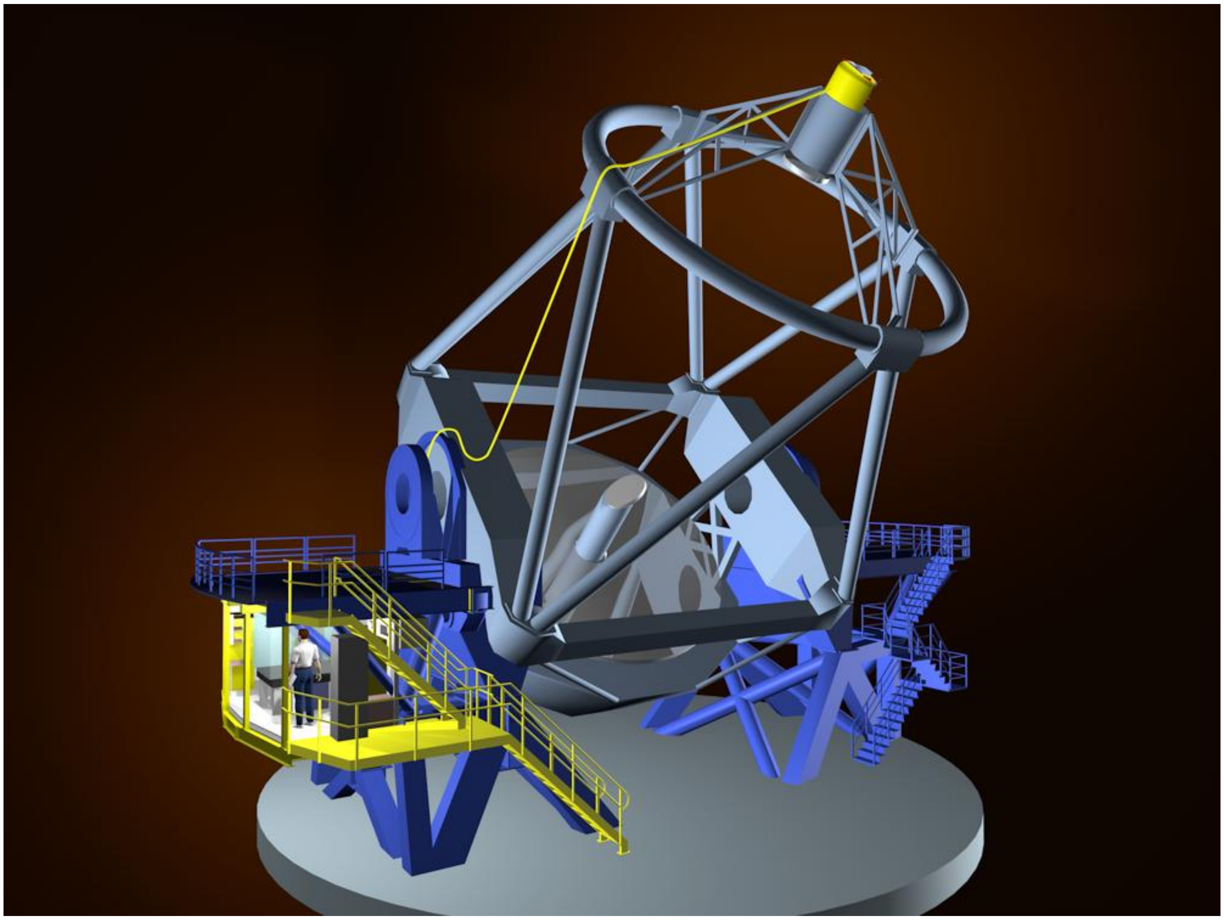

Figure 1: The LGSF on UT4 has a light-tight Laser Clean Room class 10000 built under the Nasmyth A platform, where the PARSEC laser and the electronics cabinets are hosted in a controlled atmosphere. A fibre cable containing 5 single mode Photonic Crystal Fibres carries the laser light up to the lunch telescope, delivering a diffraction liited beam. The Launch Telescope is hosted behind the secondary mirror, together with beam diagnostic devices.

4.1 The PARSEC dye Laser

The PARSEC dye laser is composed of a Master oscillator ring-dye laser producing 2W CW at 589nm, with 20 MHz linewidth, and a power amplifier producing routinely 13 W CW. The dye solution used is Rodhamine6G, and 5 Coherent VerdiV10 lasers are used as pumps, one for the master and two for the amplifier for a total of 50W CW at 532nm. When perfectly tuned and using a fresh dye solution, PARSEC has produced up to 24W CW with 50W CW of pump power input, demonstrating 48% conversion efficiency (26% with 13W CW routine output). The Technical Specifications for the optical laser beam are:

Mode of Operation	CW
Wavelength	589.0 nm (in air), tuned and stabilised to peak of sodium D_2 line with an accuracy of ≤ ± 100 MHz (goal: ± 20 MHz)
Output Power*	≥ 10.0 W, goal: ≥ 15.0 W
Spatial Mode	TEM_{00} $M^2 \leq 1.3$, goal: $M^2 \leq 1.2$

* Equals the lower limit of the long-term power stability range.

	Beam waist location: 0 mm –10/+100 mm w.r.t. to output bezel
	Beam waist diameter[†]: 0.85 ± 0.05 mm
	Beam waist asymmetry[‡] ≤ ± 5 %
	Beam waist astigmatism[§] ≤ ± 5 %
Polarisation	Linearly polarised, ≥ 100:5 (goal ≥ 100:1)
	Maximum two polarisation planes
	If single plane: off vertical within ± 2°
	If two planes: direction orthogonal (goal: vertical and horizontal), each within ± 2°, of equal intensity within ± 15 %
Longitudinal Mode	Single-frequency, spectral linewidth (10 ms) ≤ 10 MHz FWHM
	Goal: Multiline, envelope linewidth (10 ms) ≤ 0.5 GHz FWHM
Tunability	Detuning ≥ 5 GHz. Detuning time ≤ 30 s. Retuning time ≤ 30 s
	Goal: Mode hop free tuning range ≥ 5 GHz, tuning speed ≥ 200 MHz / s
Long Term Power Stability	≤ -15 % over ≥ 72 hours (goal: ≥ 168 hrs) at full power operation
Intensity Noise	≤ 1.0 % rms (> 500 Hz)
Beam Position Stability	Pointing: ≤ 0.2 mrad rms. Lateral shift ≤ 10 µm (goal: ≤ 2 µm) rms. Both rms measured for ≥ 10 sec.
	If combined beams: colinearity ≤ 0.3 mrad rms (pointing), ≤ 14 µm (goal: ≤ 3 µm) rms (centering)
Isolation	PARSEC shall perform according to its specification even if 1 % of the PARSEC output is reflected back by the BRS

PARSEC now routinely delivers 13 W CW (10W spec), if the environment is stable. This has been not so easy to achieve.
The laser can be switched from standby to full power and viceversa, using the SW control panels and no manual intervention.
The frequency lock and the servocontrols are working fine, delivering both the power stability and beam quality requested.
The Lidar mode of operation is also working fine, PARSEC has demonstrated reliable operation.
The ordinary maintenance once/week is to be confirmed in the coming months.

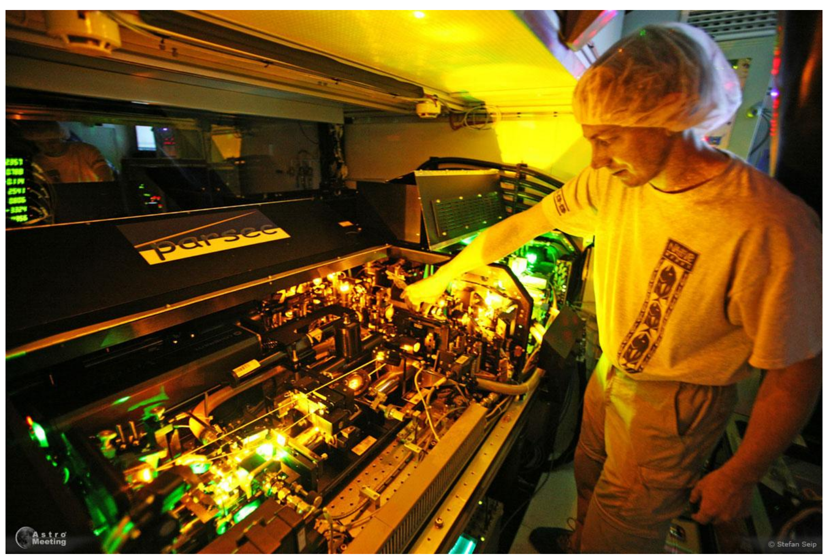

Figure 2: Ric Davies (MPE) tuning the PARSEC laser installed in the Laser Clean Room on the VLT-UT4.

† at $1/e^2$ intensity points.
‡ ratio of the beam waist diameter in the vertical direction to the waist diameter in the horizontal direction.
§ difference between the beam waist positions in the vertical and horizontal direction, normalized to the Rayleigh range for the equivalent radial-symmetric beam.

4.2 The Fiber Relay

The solid core, single mode Photonic Crystal Fibre with 14.5 μm Mode Field Diameter has been developed together with Crystal Fibre AS (DK) and Mitsubishi Cable (Japan). Mitsubishi Cable has also provided the fire-proof cable used to host 5 PCF fibers (one used and 4 spares). The fiber Numerical Aperture is 0.04. The fibre uses index guiding and is 27.5m long.

The major obstacle in propagating high power in the fibre is the non linear effect called Stimulated Brillouin Scattering (SBS). The SBS is created by a standing sound wave in the fiber, solicited by the high electrical fields. The effect is to create a regular refractive index variation which acts as a reflective grating and sends the power backward. The threshold laser power P_{SBS} to start the SBS effect is function of the Mode Field Area, A_{core}, of the fibre length L_{fibre}, and of the laser linewidth $\delta\nu_{laser}$. Hence to propagate 10W CW via the fiber we have enlarged the Mode Field Area using a solid core PCF, and broadened the 20 MHz PARSEC line using a high power modulator based on Stoichiometric Lithium Tantalate.

(1)
$$P_{SBS}(\delta\nu_{laser}) := \frac{42 \cdot A_{core}}{g_{SBS\_Max} \cdot \left(\frac{\delta\nu_{SBS\_SiO}}{\delta\nu_{SBS\_SiO} + \delta\nu_{laser}} \right) \cdot L_{fibre}}$$

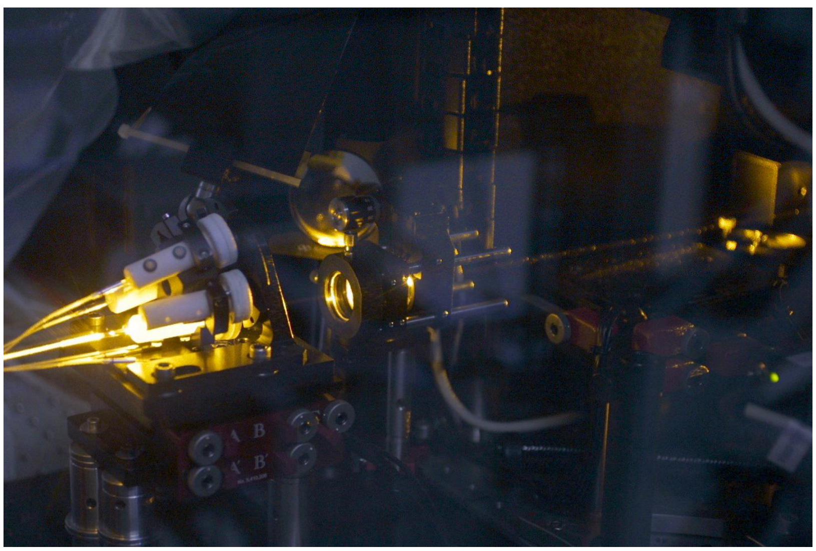

Figure 3: high power ceramic fiber couplers used to focus the PARSEC laser beam (right) into the PCF optical fibre (left). Note that spare fibres and couplers are mounted on a revolving unit.

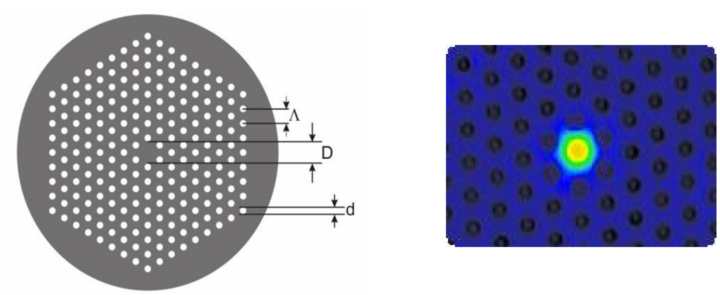

Figure 4: PCF geometry (left), and image of the laser beam (above) guided in the solid core at the PCF center. A log scale has been used to display the laser beam wings intensities.

The PCF has achieved 73% throughput including coupling losses and fibre losses, with an output beam quality of M^2=1.05. The input coupling losses are very sensitive to the laser beam quality. A perfect laser beam with M^2~1.05 would be an asset. In this case 87% throughputs have been measured at high power.

The fiber ends have been collapsed and anti-reflection coated with hardened laser coatings at 589nm. Custom borosilicate glass ferrules have been used to avoid contamination of the fibre ends from metallic particles, at high power levels. No glue can be used at the fiber termination.

We have sealed the ceramic supporting the fiber coupling lens in order to avoid that the electrostatically charged fiber end attracts dust or oil or metallic particles. This experience we had during the development period.

Alignment mismatches between the laser beam and the fiber coupler can generate overheating; hence we have removed the jitter introducing ad hoc tip-tilt correction systems before the fiber input.

Overheating of the fiber end, and eventually permanent damage, can also be generated by poor beam quality in the laser input beam, and by low air pressure at high altitude. Specific cooling with refrigerants has to be implemented in these cases.

4.3 The Launch Telescope

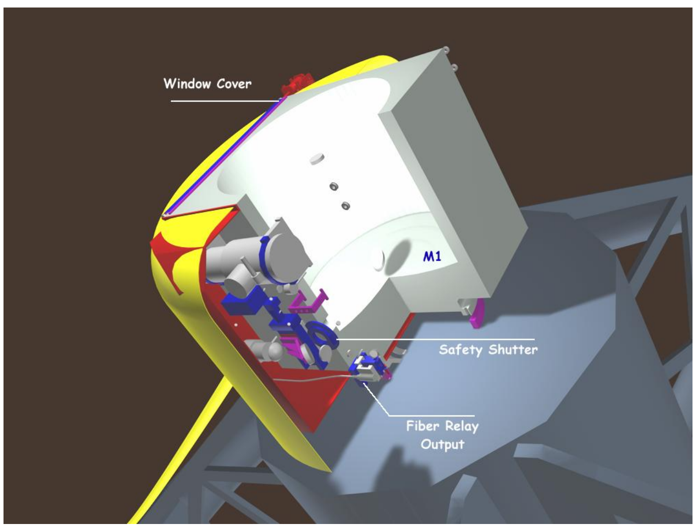

Figure 5: Launch Telescope System, including the diagnostics. An inner structure in Carbon Fiber Reinforced Plastic (CFRP) holds the secondary mirror in place aboove the primary. An outer structure in aluminium shields the telescope from wind, and supports the diagnostic devices on the side. The fibre end is placed at the focal plane of the Launch Telescope.

For reasons of allowed volume and weight, we had to implement an f/1 reflective launch telescope (LT). The useful aperture diameter is 500mm. The Launch Telescope is a 12.5 beam expander, with confocal f/1 parabolas. It has special reflective and antireflective coatings, which can be chemically removed for recoating, without having to repolish the optical parts.

The telescope optical performance is diffraction limited, with 50 nm rms wavefront error in the inner 360mm diameter of the pupil (beam waist diameter).
Its central obstruction has been kept to 0.5% of the full aperture area. We have spotted during commissioning a problem at lower temperatures of the M1 supports, which were generating print-through, and a stress of them. This generated a lower than expected optical quality, with an LGS spot size of 2.2 arcsec. This is being fixed at the time of this writing.

The telescope mechanical performance is >120 Hz of first resonance frequency, with a weight of 150 kg, including 42 kg of diagnostics.
The fiber output is positioned at the focal plane of the Launch telescope optics, mounted on a Physik Instrumente Nanocube to be used for the LGS jitter control loop.

5 FIRST LIGHT

After the First Light on January 28th, the Adaptive Optics loops have been closed on LGS on February 8 and 9, with the instruments NACO and SINFONI. The LGSF Commissioning has progressed in May, with the LT pointing model, the return flux and Lidar measurements, the LGS jitter loop performance measurements, the uplink scattering performances.

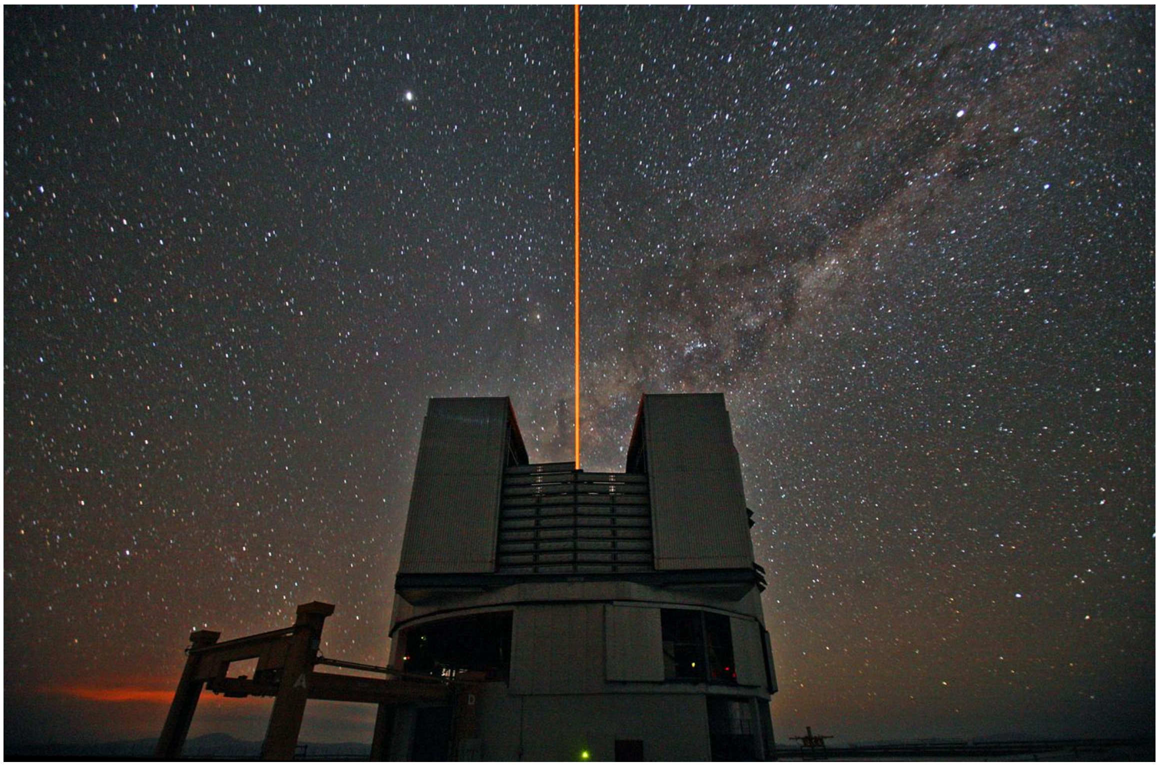

Figure 6: First Light with UT4, January 28th 2006. On February 8th and 9th we closed the LGS-AO loops with NACO and Sinfoni.

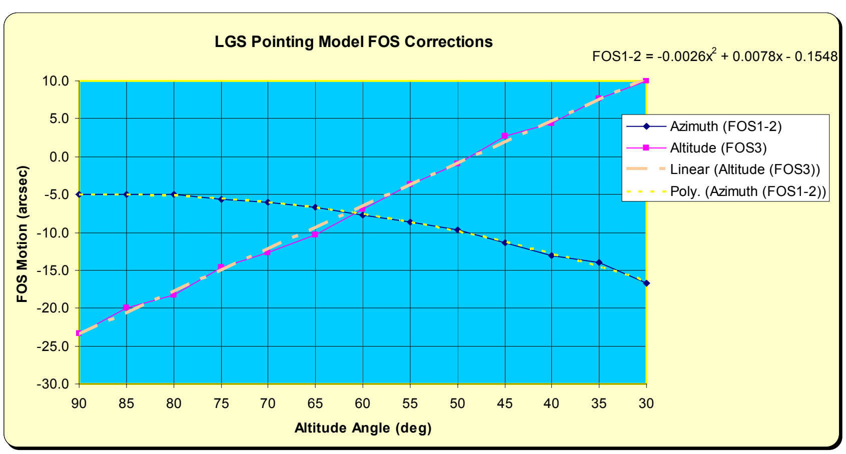

Figure 7: LTS pointing model results

The LGS pointing model has been tested (left). The Altitude and Azimuth flexures of the UT4 are well within the range of the linear actuators of the fiber positioner, and can be automatically corrected. The hysteresis levels are negligible.

We have subsequently made the pointing model in closed loop with AO, looking at the DC component of the jitter loop actuator at various pointing altitudes. This method has proven more accurate. .

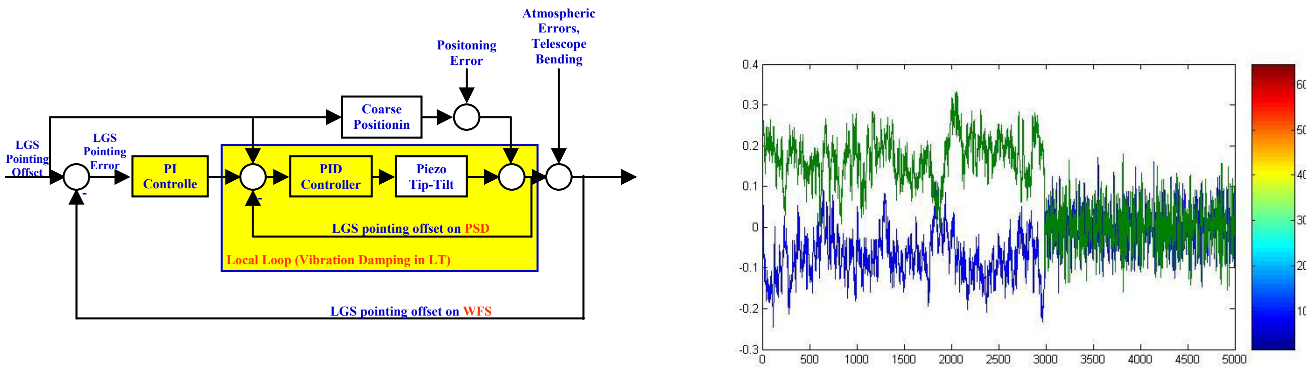

Figure 8: Schematic description of the LGS jitter loop (left) and experimental results between open and closed loop (right). The LGS jitter residual rms is <0.09 arcsec, which is the specification.

The LGS jitter loop has been tested with NACO and Sinfoni and it is performing within specifications. By design, the correction using an uplink actuator suffers from the extra time-delay of the uplink and downlink times. This required a special design for the jitter loop controller, considering that the AO system refresh rate is 480 Hz. If smaller LGS jitter residuals are sought, it is better to stabilize the LGS with an actuator in front of the wavefront sensor (WFS). This might be the case for curvature AO systems.

We have built in PARSEC a Lidar function which uses an APD module in the AO WFS to collect the return photons and derive the relative sodium density. We have also tested the concept of a Laser Guide Star Monitoring system, which uses a side telescope to derive the Sodium profile and the uplink beam scattering levels in the first 20 km. We did not find much scattering signal above 20 km at Cerro Paranal, during 5 observing nights in May. Further analysis of the data to derive Mie and Rayleigh scattering is progressing.

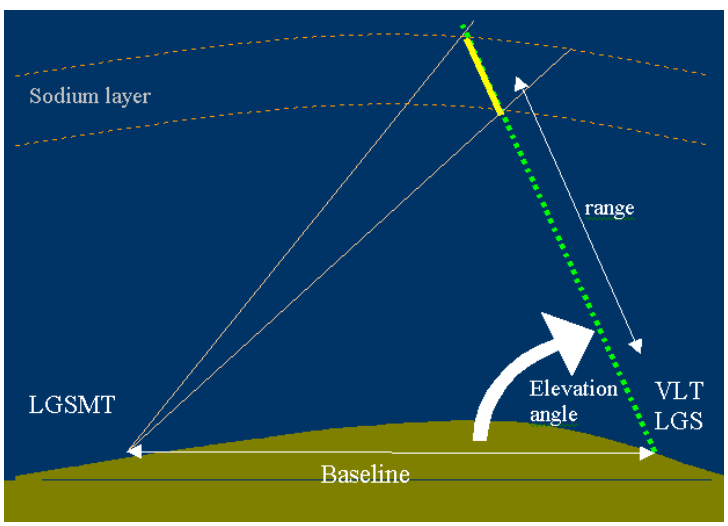

Figure 9: MGS Monitoring Telescope. It has been validated together with the LGSF Lidar function with simultaneous observations.

The simultaneous observations obtained with the LGSMT and the Lidar mode of the LGSF have validated the two methods, on May 6th 2006. We have observed for 1800 seconds simultaneously.

The monitoring telescope is an 11 inch Celestron, with a 12 bit CCD detector and an image scale of 0.66"/pxl, and a field of view of 14.3x11 arcmin. We found that a larger FoV is desirable. The baseline was 2250m, from UT4.

To calibrate the LGS flux we have used Photometric Standards on the LGSM, and the Johnson V filter. We have consistently obtained 2 M phot/sec/m^2, or an equivalent V-magnitude of 8.8, and estimated the sodium density to 3.

The estimated Sodium column density is 3×10^{13} m^{-2}, which is a value consistent with the reported Mesospheric Sodium seasonal variations for the Southern Emisphere.

The measured scattering flux from the uplink beam, per unit meter of lengtg has been obtained with the LGSMT; it is fitted by the formula $S = 3 \times 10^{12} - H \times 10^{8}$ phot/s/sterad/m, where H is the altitude in m.

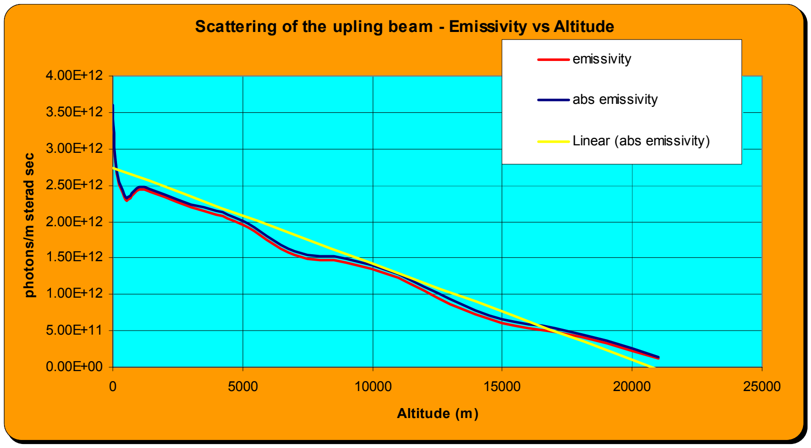

Figure 10: Photon scattering from the uplink laser beam. The units published allow to calculate the flux received from a ground telescope.

The deviations of the measured curve from the fitting is attributed to variations in the Mie scattering with altitude, the analysis of the data is in progress.

The derived formula allows to compute the extent of fratricide effects in multiple laser beam projected monostatically. The fratricide effect produces an increased background in the Wavefront Sensor subapertures of multiple LGS systems.

A comparison with numerical simulations results will be done by our group and reported in a future paper. The image of the Mesospheric plume seen from the LGSMT is shown in Figure 10.

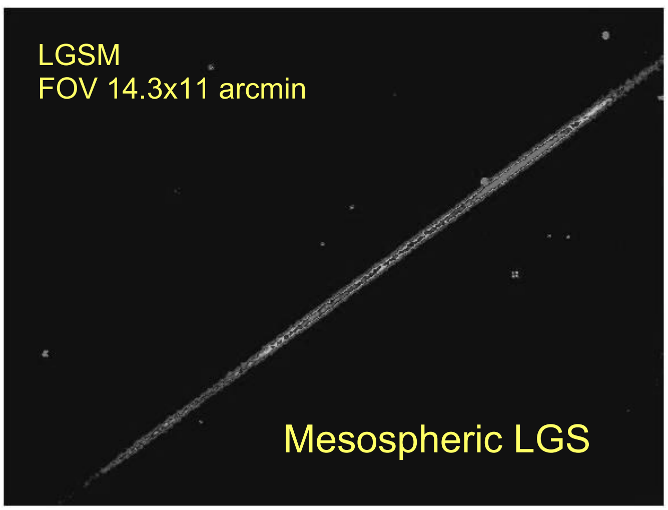

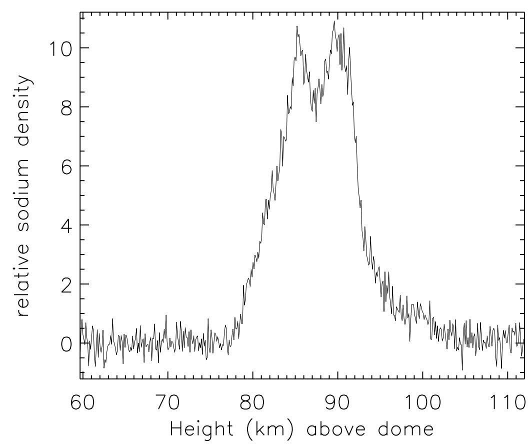

Figure 11: image of the LGS mesospheric plume, seen from the LGSMT (left). A double peak profile is observed, and confirmed by the contemporary Lidar profile obtained with the LGSF (right).

The continuous sequence of Sodium profile measurements reveal a continuous change of the median profile height, with rates up to 120m/min. This is shown in Figure 12.

25 minutes of continuous Mesospheric Sodium abundance data, sampled every ten seconds, is shown in Figure 13. These LGSMT data match very well with the data obtained by the Lidar system, at sampling rates of 90 seconds.
An increase in Sodium density, appears in the data at about 89 km of altitude a few minutes before the end of the observations.

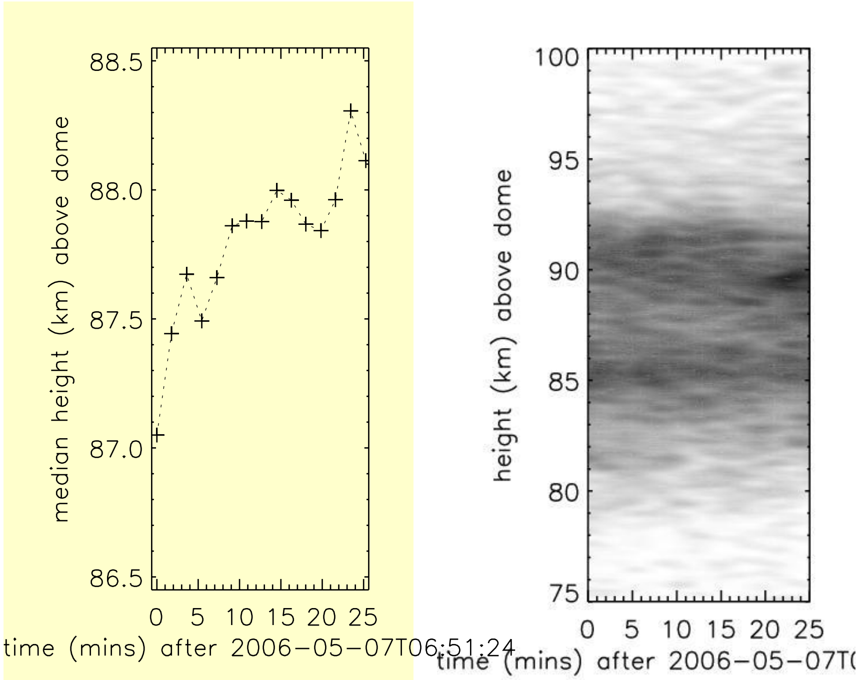

Figure 12: Variation of the median height of the Sodium profile vs time (left), derived from the LGSF Lidar data obtained over 25 minute. Darker in the colour table indicates higher densities. Note the increase in Sodium density at 89 km above the dome, around the 20th minute.

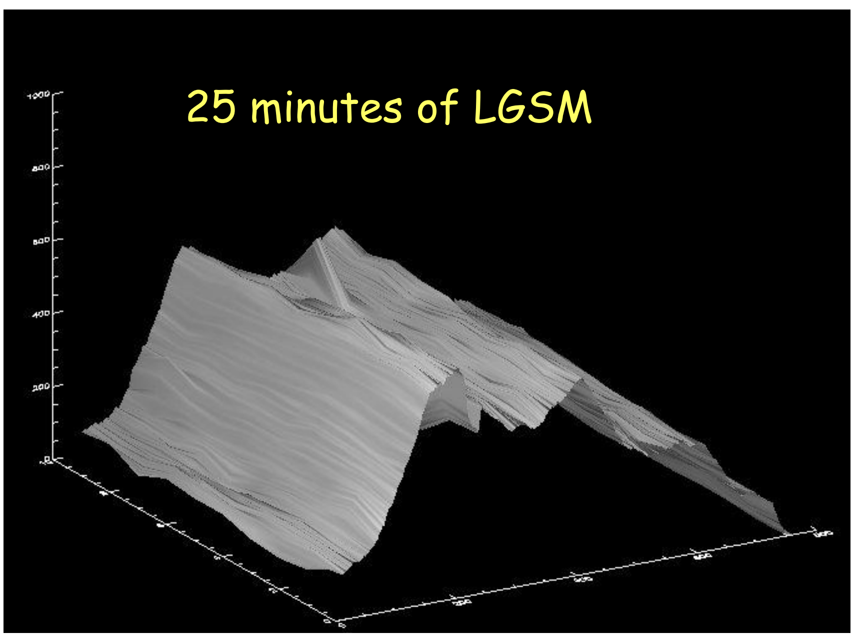

Figure 13: LGSM telescope sodium profile data obtained from the observed Sodium plume. Density is on the vertical axis. The height axis is from right (lower altitude) to the left of the horizontal axis. The time axis is the one connecting the vertical axis with the horizontal. Time is increasing approaching the vertical axis. Note the increase in Sodium density appearing toward the end of the period, in the middle of the range, likely due to a spurious Sodium layer.

6 CONCLUSIONS

The ESO LGSF has been installed on the UT4, had its first Light on January 28th 2006 and is undergoing Commissioning phases. It has not been a walk

We confirm what has been reported by other groups with LGS systems, retrofitting an existing telescope obliges to design compromises and introduces extra complications in the system. A lot of useful lessons have been learned and will be used also in the next generation multiple LGS systems for the VLT.

The LGS Pointing, jitter correction and return flux are well within the technical specification.

The undergoing commissioning runs are aiming at offering the LGS-AO systems to the community in the next Observing period in the fall of 2006. ESO successfully closed the LGS-AO loops, with the NACO and Sinfoni systems.

The latter is a curvature WFS system, and it is the first time that an LGS-AO loop is demonstrated with such systems.